

Effect of Surface Micro-textures on the Bonding Strength of PTFE Liner

Rui Peng^{1,a}, Peiyun Zhang^{1,b}, Yalin Chen^{2,c}, Yihang Zhu^{1,d},
Xiaobin Cao^{1,e} and Xijun Hua^{1,f}

¹School of Mechanical Engineering, Jiangsu University, Zhenjiang 212013, China

²Jiangsu CCTY Bearing Co. Ltd, Zhenjiang 212013, China

a. pengrui_jy@163.com, b.pyzh@ujs.edu.cn, c. chen@ccvi.com.cn, d. zyhm324@163.com,
e. 2044213592@qq.com, f. xjhua@ujs.edu.cn

Keywords: Micro-textures, PTFE liner, bonding strength, numerical simulation, tensile test.

Abstract: To improve the bonding performance and service life of PTFE liner and substrate, laser micro-textures technology was applied to the micro-modeling treatment of substrate surface to explore the influence of micro-textures density on the bonding performance of PTFE liner. Substrate-liner geometric models were established by finite element software, and the damage of adhesive layer, the tensile stress of liner, load-displacement relationship, and maximum peeling force of liner were obtained by numerical simulation. Textured substrates were prepared by Nd: YAG laser and the bonding performance was tested by a universal tensile testing machine to verify simulation results. The results of numerical simulation showed, when SDEG=0.85, The maximum peeling force increased with the increase of textures density, and the maximum peel force was 33N when the density was 34.7%. The performance test results showed a similar trend to the simulation results, in which the peeling force of the 40% density surface liner was increased by 46.15% compared with the smooth one, thus supporting the simulation results. This shows that the surface laser micro-textures has a significant impact on the bonding strength of the liner. The peeling force of PTFE liner increases with the increase of textures density, and the higher density, the better bonding performance between substrate and liner.

1. Introduction

The self-lubricating joint bearing is composed of an outer ring with an inner spherical surface and an inner ring with an outer spherical surface. The inner spherical surface of the outer ring is bonded with a layer of self-lubricating liner. Because of its simple structure, impact resistance, high load-bearing capacity, and long service life, it is widely used in aerospace, engineering machinery, water conservancy, military, and other fields[1-3]. PTFE braided composite materials are widely used as a self-lubricating liner due to its excellent anti-friction and anti-wear properties[4-7]. In the working process of the joint bearing, the liner often falls off due to the severe friction between the inner ring and the outer ring, which in turn leads to the failure of the self-lubricating joint bearing[8-10].

Therefore, it is of great significance to improve the bonding performance between the self-lubricating liner and the bearing substrate.

Scholars at home and abroad have carried out preliminary research on improving the bonding performance of self-lubricating liner and substrate. Liang Xia et al. modified PTFE/aramid composite liner with acrylamide, phosphate ester coupling agents, and glycerol ethers. The study found that the adhesive performance of the modified liner and the bearing was significantly improved[11] Jia Z. N. et al. found that changing the surface roughness of the substrate can directly affect the bonding performance of the fabric liner so that the liner can obtain better peel strength and shear strength[12]. M. S. Piskarev et al. used DC discharge to treat the PTFE liner. The results showed that the surface contact angle of the liner after the discharge treatment was significantly reduced, which effectively improved the bonding performance between the liner and the substrate[13]. Xia Bin proposed a new bonding and curing process to improve the bonding strength between the self-lubricating liner and the substrate[14].

In recent years, laser surface micro-textures technology has gradually been applied to the surface of tools, cylinder liners, bearings, die, and other parts due to its advantages of high efficiency, precision, and environmental protection. By preparing micro-textures on the surface, the lubrication effect of parts is improved and the service life is prolonged[15-18].

However, there are few reports about the laser micro-textures technology used to improve the bonding performance of joint bearings and liner. In this paper, the substrate-PTFE liner is taken as an example, the surface of the substrate is textured, and the effect of laser micro-textures density on the bonding performance of the substrate-PTFE liner is studied by numerical simulation and experimental verification. To improve the adhesive strength of the inner gasket of the joint bearing to provide a technical basis.

2. Experiment Part

2.1. Numerical Simulation

In this paper, a bilinear constitutive model based on the Traction-Separation material model is used to describe the failure mode of the cohesive element material[19]. The description method of the bilinear constitutive model is shown in Figure.1.

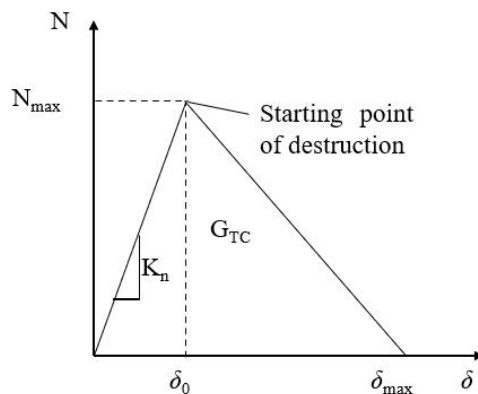


Figure 1: Bilinear constitutive model.

N_{max} —Maximum tensile force; K_n —Cohesive unit stiffness; δ_0 —Unit displacement at maximum tensile force; δ_{max} —Relative displacement when the interface is completely destroyed; G_{TC} —The fracture energy released by the complete destruction of the interface. G_{TC} can be expressed by formula (1):

$$G_{TC} = \frac{1}{2} \delta_{\max} N_{\max} \quad (1)$$

Kn can be expressed by formula (2):

$$K_n = \frac{N_{\max}}{\delta_0} \quad (2)$$

Table 1 shows the material performance parameters of the PTFE liner and adhesive layer used in the simulation.

Table 1: Property parameters of materials.

Key parameters	PTFE liner[20]	3M DP 460[21]
Young's modulus(MPa)	1300	3000
Poisson ratio	0.4	
Tensile strength(MPa)	25	20
Percentage of breaking elongation(%)	250-500	
Shear strength(MPa)		15
Shear modulus of elasticity(MPa)		1154
Normal fracture energy(N/mm)		0.3
Shear fracture energy(N/mm)		0.52

The textured substrate was prepared by three-dimensional modeling software, as shown in Figure.2. The finite element simulation software ABAQUS is used to establish the substrate-liner geometric model as shown in Figure.3. The upper layer is PTFE liner layer (L=80mm, h=2mm), the middle layer is 3M DP 460 equivalent adhesive layer (initial thickness 0.2mm), the lower layer is the substrate layer (L=80mm, h=8mm) and the viscosity coefficient of the middle layer is defined as 0.01. The geometric model is meshed in the form of a two-dimensional four-node (COH2D4) cohesive unit, the normal vertical displacement boundary condition is applied to the upper right corner of the pad, and the bottom surface of the substrate is a fixed constraint. When SDEG=1, the cohesion unit in the Viscous Regularization interface will be deleted after failure. To facilitate the observation of the simulation results, this article defines the coefficient in Max Degradation as 0.85, which means that when SDEG=0.85, the user-defined cohesion unit is considered to have completely failed.



Figure 2: Surface morphology.

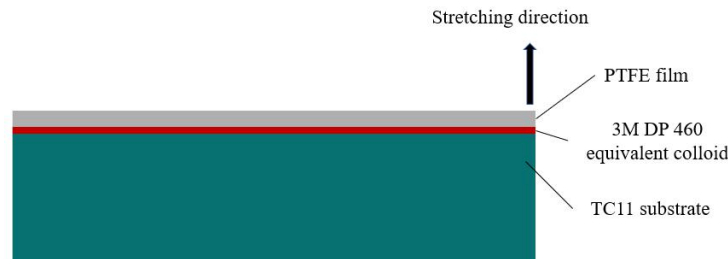


Figure 3: Geometric model of matrix-liner.

2.2. Tensile Test

Nd: YAG laser (Figure.4) was used to process the micro-textures (diameter $110\mu\text{m}$, depth $27\mu\text{m}$, and 10% and 40% in density) on the surface of the substrate. The micro-textures morphology is shown in (Figure.5). The processing parameters: current 20A, pulse width 70ns, and pulse repetition times 10 times[22].



Figure 4: YAG laser equipment.

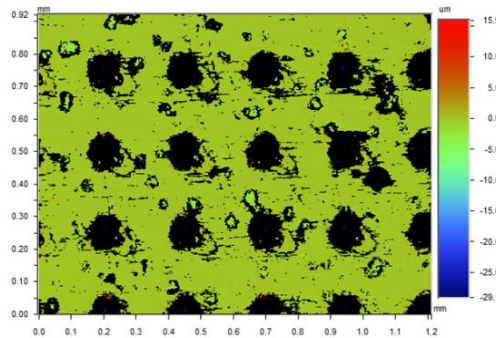


Figure 5: Micro-textures morphology.

Coat the adhesive on the surface of the substrate and the PTFE liner and keep the pressure for a certain time. After the sample is completely cured, place it in a high-temperature heating box and heat it for 2 hours, keep the temperature in the box at 150°C , and take out the sample for a tensile peel test (Figure.6).



Figure 6: Peel test.

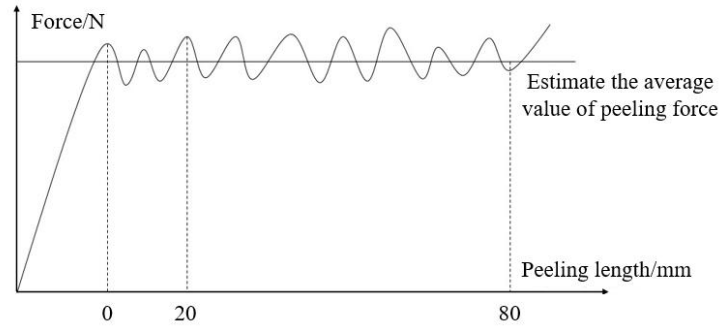


Figure 7: Peeling force-peeling length curve.

The peel force-peel length curve (Figure.7) is used to estimate the average peel force, and the maximum peel force is determined by the maximum peak value of the curve, with N as the unit. The tensile specimen is a rectangular block of 120mm×30mm×10mm. In the calculation process, it is necessary to remove the clamping length of 20mm and the pre-stretching displacement of 20mm at the beginning of stretching, and the effective stretch length of 80mm is used to calculate the peel strength value. Calculation method as shown in formula (3).

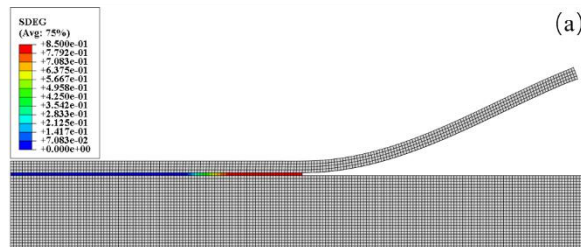
$$\sigma_T = F/B \quad (3)$$

σ_T —Peel strength(N/mm); F—Peel force(N); B—Sample width(mm).

3. Results and Analysis

3.1. The Effect of Density on Bonding Strength

To explore the effect of micro-textures density on the bonding performance of the substrate-liner interface, micro-textures with a density of 12.6%, 19.6%, and 34.7% were designed on the surface of the substrate. The tensile simulation results are shown in Fig.8 and 9. Compared with smooth sample (Figure.9(a)), the tensile stress of the substrate surface liner with textures density of 12.6% (Figure.9(b)), 19.6% (Figure.9(c)) and 34.7% (Figure.9(d)) increased by 39.55%, 47.63% and 52.86%, respectively. It can be seen from the above that the greater the tensile stress of the liner, the higher the bonding strength. Therefore, within the scope of the research parameters set in this paper, the tensile stress of the substrate surface liner increases with the increase of textures density, and the bonding strength of the higher density textured substrate surface liner is higher.



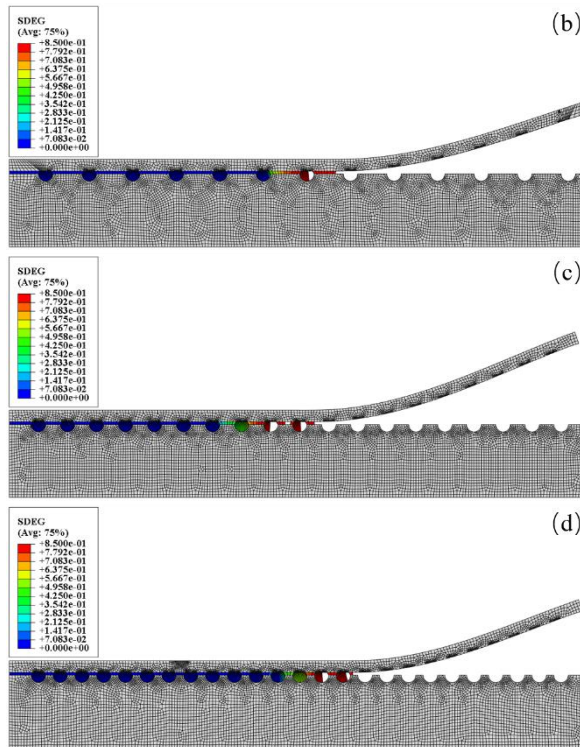
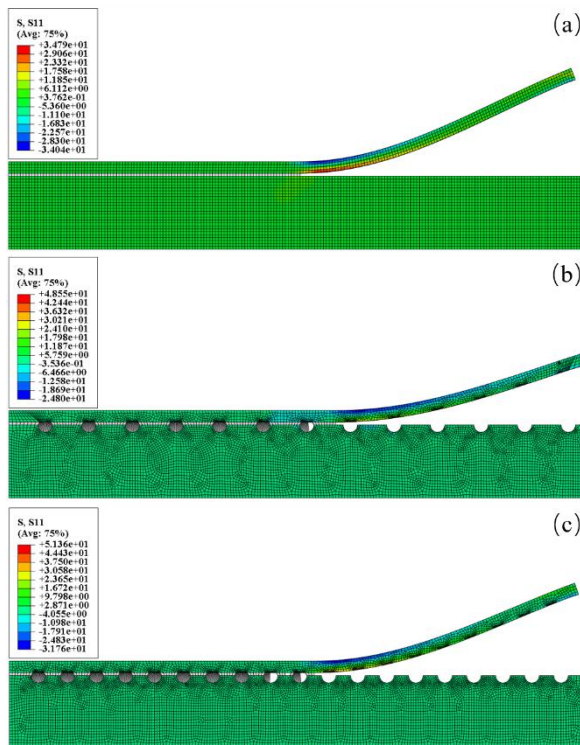


Figure 8: Damage of adhesive layer.



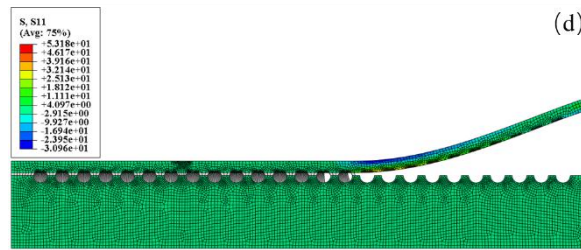


Figure 9: Tensile stress of liner.

The maximum peeling force of the substrate surface liner treated with different density textures has increased to varying degrees. With the increase of textures density, the maximum peeling force shows an increasing trend. When the textures density is 34.7%, the maximum peel force is about 33N, which is a 65% increase compared to smooth sample, as shown in Figure.10 and 11. The textured treatment on the surface of the substrate increases the specific surface area of the substrate-liner contact and increases the surface roughness. At this time, the cement can fully wet the metal surface and penetrate into the metal void. The cement can produce greater bite force with the metal matrix; on the other hand, the higher density textures can store more adhesive, provide greater shear force during the stretching process, and make the adhesive layer difficult to fall off. The interface bonding strength is further enhanced.

The numerical simulation output results can show that within the parameters studied in this paper, the micro-textures can increase the peeling force of the liner, and the bonding strength increases with the increase of the density of the textures.

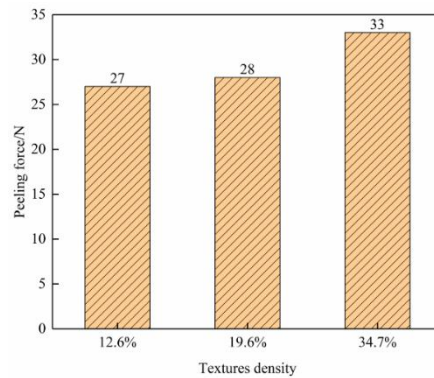


Figure 10: Load-displacement relationship.

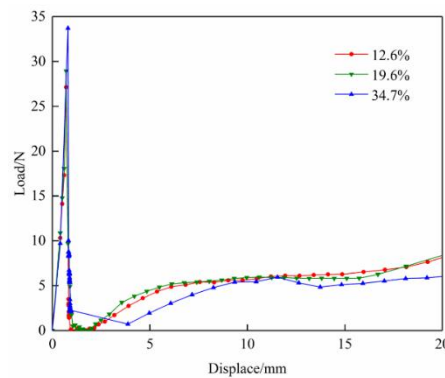


Figure 11: Film peeling force on the surface.

3.2. Bonding Performance Test

The test results are shown in Figure.12. After the sample undergoes the peel test, a part of the colloid remains on the surface of the sample, and the other part of the colloid is separated with the liner. The adhesive failure mode is mainly a mixed form of interface failure and cohesive failure, and some adhesive failures. It occurs inside the glue layer, and the other part occurs on the surface of the substrate.

The results of the bonding performance test show that the laser micro-textures can effectively enhance the bonding strength of the substrate-liner, and the peeling force increases with the increase of the density of the textures; compared to the smooth sample, the peeling force of the 10% sample increased by 35.90%, and the peeling force of the liner on the surface of the 40% density sample increased by 46.15%, as shown in Figure.13. Because the micro-textures increases the effective contact surface area of the substrate surface and the completely softened adhesive can fully contact the substrate surface, penetrate into the voids on the substrate surface, and produce strong physical adsorption and mechanical occlusion. The adhesive that penetrates into the textures can generate stronger shear force during the stretching and peeling process, effectively enhancing the interface bonding strength. During the research process, it was found that although the numerical simulation and the actual test data have certain errors, the increasing trend of the sample surface peel force with the increase of textures density is consistent with the simulation results, thus verifying the accuracy of the numerical simulation.



Figure 12: Specimens after degumming.

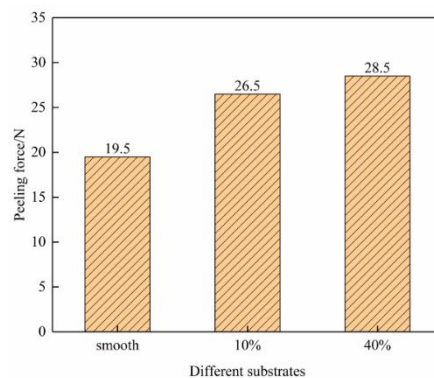


Figure 13: Film peeling force on the surface.

4. Conclusions

The bonding strength of the liner increases with the increase in textures density. When the density is 34.7%, the maximum peel force of the liner is about 33N, which is 65% higher than that of the smooth sample, showing the best bonding performance.

The results of the bonding performance test and the numerical simulation showed the same trend. The maximum peeling force increased with the increase of textures density. The peeling force of the surface liner of the 40% density sample was increased by 46.15% compared with the smooth sample. It fully shows that the surface micro-textures can effectively improve the bonding performance of the substrate-PTFE liner.

Laser surface micro-textures technology provides a theoretical basis and technical guidance for parts that require improved bonding performance, such as surface liner and engineering coatings of joint bearings.

Acknowledgments

This work was financially supported by National Natural Science Foundation of China (No. 51975252); Project of Scientific Research Innovation Plan for Postgraduates in Jiangsu Province (NO. SJCX19_0546); Major Scientific and Technology Project of the Zhenjiang City (ZD2018001); High-technology Research Key Laboratory Project of the Zhenjiang City (SS2018007), Major Scientific and Science and Technology Support Plan of the Taizhou City (TG201920).

References

- [1] SHEN Xue-jin, CAO Lei, CHEN You-guang, et al. Research Status and Prospect of Spherical Plain Bearings with Self-lubricating Fabric Liner[J]. *Bearing*, 2009, (3): 57-61.
- [2] Ivanov V. A, Zakharychev S. P. Self-lubricating bearings based on compound epoxy fluoroplastics[J]. *Russian Engineering Research*, 2017, 37(3): 206-210.
- [3] Zhang Qing-long, Hu Zhan-qi, Yang Yu-lin, et al. Investigation of the roller swaging process for self-lubricating spherical plain bearings assembly[J]. *Journal of Materials Processing Technology*, 2017, 241: 36-45.
- [4] XIE Xuan, YIN Bi-feng, HUA Xi-jun, et al. Research on Sliding Friction Properties of PTFE/GCr15 Laser Textured Surface under Grease Lubrication[J]. *Surface Technology*, 2019, 48(8): 77-82.
- [5] XIANG Ding-han, PAN Qing-lin, YAO Zheng-jun. Friction and Wear Behavior of Polytetrafluoroethylene Fabric Composite Spherical Bearing in Swaying[J]. *Tribology*, 2003, 23(1): 72-75.
- [6] QIU Ming, ZHOU Zhan-sheng, ZHOU Da-wei, et al. Tribological Properties of Self-Lubricating Spherical Plain Bearings with PTFE/PPS Fabric Liners[J]. *Tribology*, 2018, 38(5): 547-553.
- [7] ZHU Jian-jun, XIE Fang, Dwyer-Joyce RS. PEEK Composites as Self-Lubricating Bush Materials for Articulating Revolute Pin Joints[J]. *Polymers*, 2020, 12(3).
- [8] BAI Yao-xing, QIU Ming, LI Ying-chu, et al. Study status and development of the wear failure of spherical plain bearing[J]. *Modern manufacturing engineering*, 2012, (4): 138-142.
- [9] DUAN Hong-yu, LIU Hong-yu, ZHU Lin-lin. Failure Analysis and Optimal Design for Self-Lubricating Spherical Plain Bearings Based on Workbench[J]. *Bearing*, 2016, (9): 52-55.
- [10] XUE Ya-hong, CHEN Ji-gang, GUO Su-min, et al. Finite element simulation and experimental test of the wear behavior for self-lubricating spherical plain bearings[J]. *Friction*, 2018, 6(3): 297-306.
- [11] LIANG Xia, QIU Ming, LI Ying-chun, et al. Effects of liner modification on the bonding behavior and tribological properties of self-lubricating spherical plain bearings[J]. *Modern manufacturing engineering*, 2017, (3): 7-11.
- [12] JIA Zhi-ning, HAO Cai-zhe, HAN Chao. Influences of Surface Roughness of Steel Substrate on Bond Strength of Fiber Woven Composite[J]. *Applied Mechanics and Materials*, 2014, 481: 258-263.
- [13] Piskarev M. S, Gil ' man A. B, Shmakova N. A, et al. Direct-current discharge treatment of polytetrafluoroethylene films[J]. *High Energy Chemistry*, 2009, 42(2): 137-140.
- [14] XIA Bin, Research of a new type of spherical plain bearing adhesive curing process parameters[D]. *Qinhuangdao: Yanshan University*, 2015.
- [15] PENG Rui, ZHANG Pei-yun, TIAN Zhi-xiang, et al. Effect of textured DLC coatings on tribological properties of titanium alloy under grease lubrication[J]. *Materials Research Express*, 2020, 7(6): 066408.

- [16] LIU Si-si, LIU Qiang, LIU Jin-gang, et al. Synergistic Antifriction Mechanism of Surface Micro-textured Graphite Coating on Aluminum Alloy Surface[J]. 2019, 48(8): 29-38.
- [17] HUA Xi-jun, XU Hong-shan, CHEN Ya-lin, et al. Numerical analysis on lubrication performance of laser micro-textured roller bearings[J]. Surface Technology, 2018, 47(3): 29-38.
- [18] Pakuła D, Staszuk M, Dziekońska M, et al. Laser micro-texturing of sintered tool materials surface[J]. Materials, 2019, 12(19).
- [19] Watson Brock, Liao Chi-Hsiang, Worswick Michael J, et al. Mode I traction-separation measured using rigid double cantilever beam applied to structural adhesive[J]. Journal of Adhesion, 2018, 96(8): 717-737.
- [20] Xu Y. J, Wang Z. J, Wu G. D, et al. Density effect of PTFE-copper powder metallurgy liner material on the perforation performance of shaped charge jets[J]. Strength of Materials, 2019, 51(4): 616-623.
- [21] Kim Hyun-Bum, Nishida Tomohisa, Oguma Hiroyuki, et al. Shear strength of an aluminum alloy bonded with a DP-460 adhesive: single lap-shear joints[J]. Journal of Adhesion and Interface, 2020, 21(1).
- [22] FU Yong-hong, LIU Qiang-xian, YE Yun-xia, et al. Research on Laser Surface Micro Texturing Processing of Single Pulse Intervals[J]. Chinese Journal of Lasers, 2015, 42(12): 98-105.